Exchange interactions and magnetic dimension in Cu(L-alanine)$_2$

R. Calvo* and M. C. G. Passeggi
Instituto de Desarrollo Tecnologico para la Industria Química (Intec), Güemes 3450, 3000 Santa Fe, Argentina

M. A. Novak
Instituto de Fisica, Universidade Federal do Rio de Janeiro, Cidade Universitaria, Rio de Janeiro 21945, Brazil

O. G. Symko
Department of Physics, University of Utah, Salt Lake City, Utah 84112

S. B. Oseroff
Department of Physics, San Diego State University, San Diego, California 92182

O. R. Nascimento and M. C. Terrile
Instituto de Física e Química de São Carlos, Universidade de São Paulo–São Carlos, Caixa Postal 369, 13560, São Carlos, SP, Brazil

(Received 26 April 1990; revised manuscript received 18 July 1990)

A study of the magnetic properties of the copper (II) complex of the amino acid L-alanine [Cu(L-alanine)$_2$] is reported. The susceptibility of a powder sample has been measured between 0.013 and 240 K. A linear-spin-chain model with antiferromagnetic exchange coupling $J=-0.52$ K fits well the susceptibility data above 0.3 K. Room-temperature electron paramagnetic resonance (EPR) spectra of single crystals of Cu(L-alanine)$_2$ at 9 and 35 GHz show a single, exchange-narrowed resonance. The g tensor, with principal values $g_1=2.0554\pm0.0005$, $g_2=2.1064\pm0.0005$, and $g_3=2.2056\pm0.0005$, reflects the crystal structure of Cu(L-alanine)$_2$ and the electronic properties of the copper ions. The observed angular variation of the linewidth is attributed to the magnetic interactions, narrowed by the exchange coupling between copper ions, and shows a contribution characteristic of the dipole-dipole interaction in a spin system with a predominant two-dimensional spin dynamics. Considering the exchange-collapsed resonance corresponding to the two lattice sites for copper in Cu(L-alanine)$_2$, we evaluate an exchange constant $|J(AB_1)|=0.47$ K between nonequivalent copper neighbors in a spin chain, similar to the value obtained from the susceptibility data. The one-dimensional magnetic behavior suggested by the susceptibility data in Cu(L-alanine)$_2$, where the metal ions are distributed in layers, is explained by proposing that carboxylate bridges provide electronic paths for superexchange interactions between coppers. Considering the characteristics of the molecular structure of Cu(L-alanine)$_2$, the layers seem to be magnetically split off into one-dimensional zigzag ribbons. The apparent disagreement between the one-dimensional behavior suggested by the susceptibility data and the two-dimensional behavior of the spin dynamics suggested by the EPR linewidth is analyzed.

I. INTRODUCTION

Metal derivatives of amino acids are simple model systems to study properties of metal ions in proteinlike structures. Also, the possibility of having a family of compounds with a quasicontinuous distribution of structural parameters leads us to consider metal–amino acid complexes as an attractive group of materials to investigate the magnetic interactions. These compounds motivated many studies of their crystal structures, and electronic and magnetic properties, which indicate some interesting magnetic characteristics. For example, due to the magnitude of the exchange interactions in copper amino acid complexes [Cu(aa)$_2$], which are comparable to Zeeman splittings, typical in electron paramagnetic resonance (EPR) experiments, the exchange-narrowing effects are still in the regime which allows extraction of the magnitude of the exchange parameters from the EPR linewidth data. EPR and magnetic susceptibility studies of several Cu(aa)$_2$ have been reported previously.[1–5] The observed angular variation of the EPR linewidth has been shown to be strongly linked to the magnitude and magnetic dimensionality of the exchange-narrowing process.[6] In most Cu(aa)$_2$ it indicates a low-dimensional behavior, consequence of the layered arrangement of copper ions in their crystal structures, which produces a slow spin dynamics and thus strongly influences the angular dependence of the EPR linewidths. By changing the symmetry and magnetic dimensionality in a series of Cu(aa)$_2$ having small differences in the crystallographic parameters, it has been possible,[7,8] to analyze the role of some amino acid molecular fragments as paths for superexchange in-

teractions. Those findings are useful in learning about the superexchange paths between metal ions, or between metal ions and free radicals in proteins.[9]

In this paper we report magnetization measurements in powers between 0.013 and 240 K, and EPR data obtained in single crystals at two microwave frequencies, 9 and 35 GHz, for the copper derivative of the amino acid L-alanine, hereafter referred to as Cu(L-alanine)$_2$. The data are used to evaluate the exchange interactions and analyze the magnetic dimensionality of the complex. Preliminary data were reported previously.[10,11] Our EPR results are discussed in terms of the crystallographic structure of the complex[12] and are compared to those obtained by Yokoi and Ohsawa at 9 GHz.[13]

In Sec. II the experimental details and results are presented. The crystal structure of Cu(L-alanine)$_2$ is reviewed in Sec. III, where possible superexchange paths are analyzed. In Sec. IV the susceptibility data are discussed in terms of Heisenberg models in one and two dimensions, while in Sec. V we consider the EPR data. Section VI summarizes our results and conclusions in terms of the structural information and the superexchange paths between copper ions, in connection to the spin dynamics in Cu(L-alanine)$_2$.

II. EXPERIMENTAL DETAILS AND RESULTS

A. Sample preparation

Copper (II)-bis(L-alaninato), Cu($NH_2CH_3CHCO_2$)$_2$, called Cu(L-alanine)$_2$, was obtained from the reaction of a water solution of the amino acid with basic copper carbonate. Thin blue six-sided single crystals were grown from saturated solutions at room temperature. The plates are *bc* crystal planes, with well-defined $\hat{\mathbf{b}}$ axes. These easy-to-orient samples were recognized as similar to those studied before by Dijkstra[12] using x rays, by measuring the angles between the directions defined in the samples with a goniometer microscope.

B. Magnetic susceptibility measurements

A powder sample of 16 mg, packed in an epoxy sample holder 6.2 mm long and 2.5 mm in diameter, was used to perform static magnetization measurements in a field of 1 G with a superconducting quantum interference device (SQUID) magnetometer from 13 mK up to 3.85 K, inside the mixing chamber of a ^{3}He-^{4}He dilution refrigerator. Data from 1.76 to 240 K were obtained with a VTS 50 SHE susceptometer, at a field of 1 kG. Data in the two temperature ranges were scaled together. The results obtained in the full temperature range are displayed in Fig. 1 in a $\chi_m(T)$ versus $\log_{10}(T)$ plot, to emphasize the behavior in the very low-T range. It displays a rounded maximum around 0.67 K, a plateau at 0.2 K with a shoulder at 0.1 K, a minimum for the susceptibility at 0.035 K, followed by an increase of $\chi_m(T)$ at lower temperatures. Figure 2 provides a more detailed view of the behavior of $\chi_m(T)$ below 5 K. No indication of a magnetic phase transition is observed in Fig. 1 or 2. However, the broad maximum in $\chi_m(T)$ around 0.67 K points

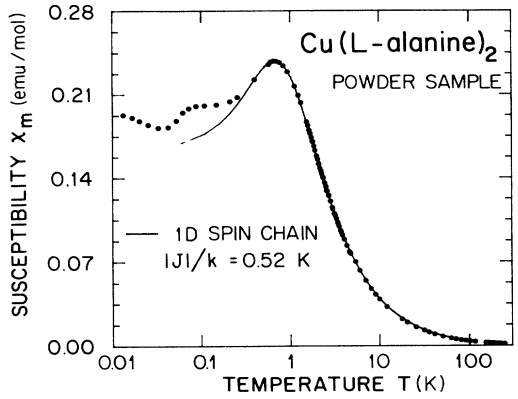

FIG. 1. Molar susceptibility $\chi_m(T)$ displayed vs $\log_{10}(T)$ in order to emphasize the low-T data. The solid line was obtained with the 1D linear chain model, using $|J|=0.52$ K.

to short-range order, typical of low-dimensional magnetic systems.[14]

C. EPR measurements

The EPR data were obtained at room temperature in single-crystal samples, using commercial spectrometers at 9 and 35 GHz. A 12-in. Hall probe-controlled rotating magnet, calibrated against a NMR fluxmeter, as well as commercial cylindrical microwave cavities, with 100 kHz field modulation, were used.

The crystals were glued to quartz or epoxy sample holders, with the $\hat{\mathbf{a}}'=\hat{\mathbf{b}}\times\hat{\mathbf{c}}$, $\hat{\mathbf{b}}$, and $\hat{\mathbf{c}}$ axes aligned along the $\hat{\mathbf{x}}$, $\hat{\mathbf{y}}$, and $\hat{\mathbf{z}}$ orthogonal axes of the sample holders, respectively. Due to size restrictions imposed by the cavities, different samples were used at 9 and 35 GHz. The orientation uncertainties were about 1° for the X-band samples, and 2° for the Q-band samples. The sample holders were positioned on the top of a pedestal inside of the microwave cavity, so the applied magnetic field **H** could be rotated in the xy, zy, and zx planes. The crystal

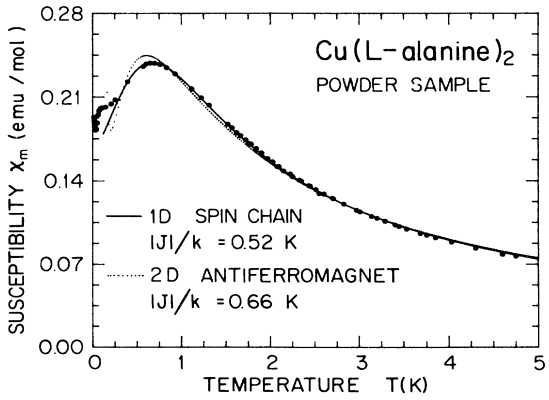

FIG. 2. Molar susceptibility $\chi_m(T)$ displayed vs T, for T below 5 K. The solid line was obtained with the linear chain model, using $|J|=0.52$ K. The dotted line was obtained with Lines' 2D model (see text).

axes in the *xy* and *yz* planes were located considering that an extreme of the angular variation of the *g* factor is required by the symmetry of Cu(L-alanine)$_2$ (see Sec. III) at the crystal $\hat{b}=\hat{y}$ axis. In the *xz* plane the crystal axes were identified by matching the angular variation observed in that plane with those found in the other two planes. The uncertainty on the orientation of the magnetic field is then limited to that of the sample in the sample holder.

The single EPR line was observed at both microwave frequencies for any orientation of **H**. The *g* factor and peak-to-peak linewidth ΔH_{pp} were measured at intervals of 5° to 10° in the three crystal planes. The angular variation of the squared *g* factors of Cu(L-alanine)$_2$ obtained for the three crystal planes, at room temperature and 9 GHz, are shown in Fig. 3. Except for minute changes in the *g* factor, the same figure is obtained from the 35-GHz data. Figure 4 compares the angular variation of ΔH_{pp} observed at 9 and 35 GHz, in the three planes. It shows that by going to higher microwave frequencies, contributions to the linewidth with a higher-order angular variation appear in the planes *a'b* and *bc*. The observed line shape is very close to Lorentzian within three linewidths from the center of the resonance, at both microwave frequencies.

III. CRYSTAL STRUCTURE AND SUPEREXCHANGE PATHS IN Cu(L-alanine)$_2$

The crystal structure of Cu(L-alanine)$_2$ was determined by Dijkstra in 1966 by two-dimensional Fourier methods.[12] The structure is monoclinic, space group $P2_1$, with $a=9.24$ Å, $b=5.05$ Å, $c=9.59$ Å, $\beta=95.2°$, and two molecules per unit cell. The positions of all nonhydrogen atoms were determined. The copper ions are in a tetragonally distorted octahedron of ligands, with two amino nitrogens and two carboxylate oxygens, in a nearly square planar transcoordination at a mean distance of ~2 Å (see Fig. 5). Oxygens O(2'') and O(4'), belonging

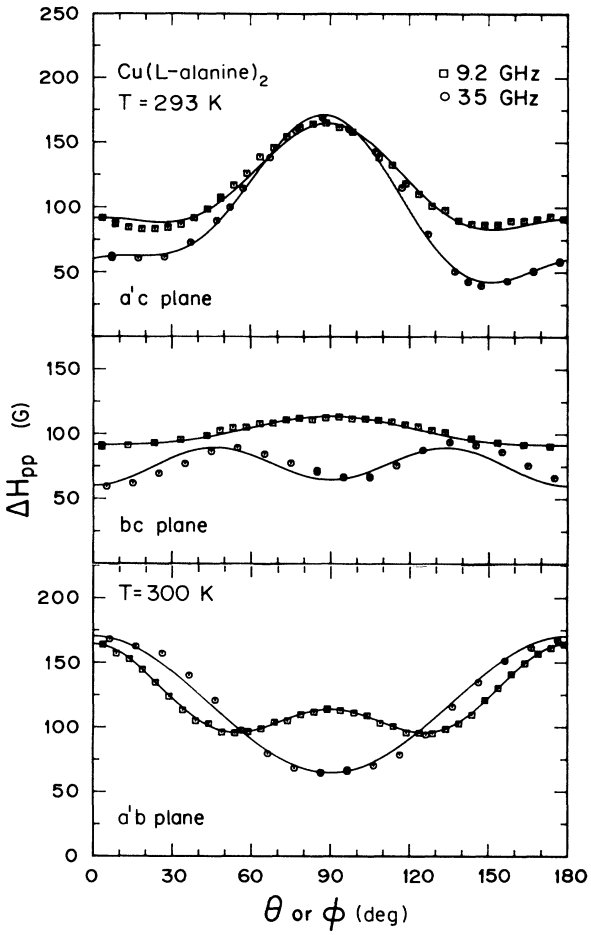

FIG. 4. Angular variation of the peak-to-peak EPR linewidth observed at 9 and 35 GHz, for a magnetic field applied in the three crystal planes *a'b*, *bc*, and *a'c* of a single-crystal sample of Cu(L-alanine)$_2$. The solid lines are obtained with Eq. (15) and the parameters given in Table II.

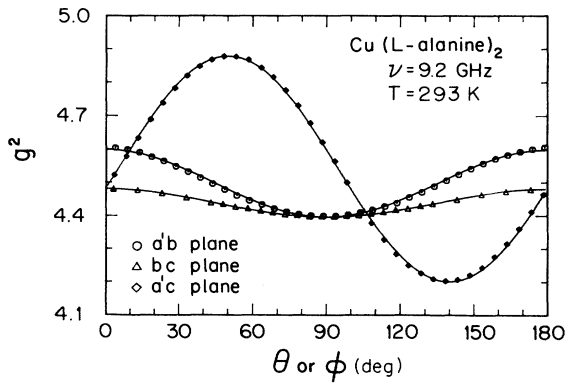

FIG. 3. Angular variation of the squared gyromagnetic factor $g^2(\theta,\Phi)$ measured at 9 GHz for the magnetic field applied in the three crystal planes *a'b*, *bc*, and *a'c* of a single crystal of Cu(L-alanine)$_2$. The solid lines are obtained with the components of g^2 given in Table I.

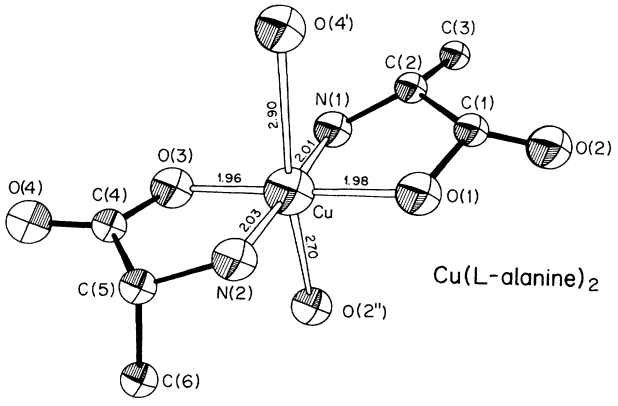

FIG. 5. The Cu(L-alanine)$_2$ molecule as obtained from the crystallographic data of Ref. 12. The distances in angstroms between neighboring atoms are indicated. There are two of these molecules per unit cell.

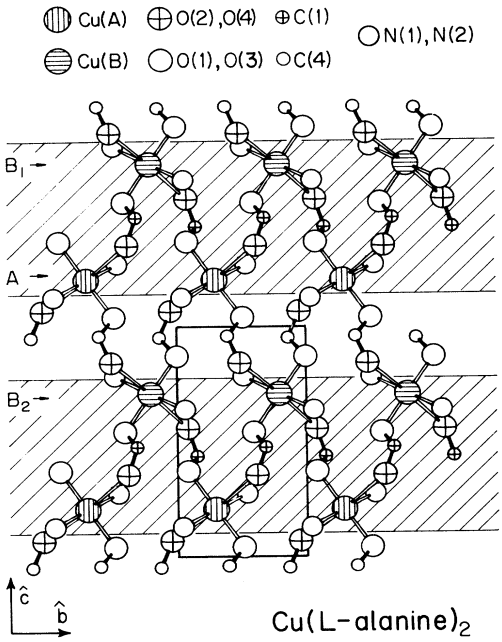

FIG. 6. Copper layers parallel to the *bc* crystal plane in Cu(L-alanine)$_2$. The names of the atoms are given in order to show the exchange paths discussed in the paper. Coppers type B_1 and B_2 are identical and only the exchange interactions between a copper type A and coppers type B_1 and B_2 are different. The 1D "ribbons" where, according to our model, most of the spin dynamics takes place when $J(AB_1) \gg J(AB_2)$, are shaded.

to carboxylate groups of neighbor molecules, occupy the apical positions of the elongated octahedron, at distances 2.70 and 2.90 Å from the copper atoms, respectively. In the unit cell of Cu(L-alanine)$_2$ there are two of these chemically identical molecules, labeled A and B, having orientations related by a 180° rotation around $\hat{\mathbf{b}}$. In Fig. 6 we show the arrangement of the copper molecules in the *bc* plane of the crystal lattice, as obtained from the data of Dijkstra.[12] The orientations of the normals to the best N_2O_2 planes of equatorial ligands to the A and B molecules in the $\hat{\mathbf{a}}' = \hat{\mathbf{b}} \times \hat{\mathbf{c}}$, $\hat{\mathbf{b}}$, $\hat{\mathbf{c}}$ system of axes are

$$(\theta_m, \Phi_m)_A = (56.1°, 34.4°)$$

and

$$(\theta_m, \Phi_m)_B = (123.9°, 145.6°) ,$$

with an angle of 124.2° between them. The coppers are arranged in layers parallel to the *bc* plane (shown in Fig. 6). Since the distance between copper layers, $a = 9.24$ Å, is twice that between copper neighbors in the same layer, we expect a low-dimensional magnetic behavior of Cu(L-alanine)[2]. Within these layers, each copper type A has six copper neighbors. Two type-A coppers are at 5.05 Å at both sides along the $\hat{\mathbf{b}}$ axis. By crystal symmetry, the corresponding superexchange paths are identical. The positions of the protons in the structure of Cu(L-alanine)$_2$ have not been determined. However, it seems that the shortest superexchange paths between equivalent copper ions involve hydrogen bridges connecting nitrogen ligands of one copper with equatorial oxygen ligands of the neighbor copper. The magnitude of the exchange interaction of one copper with the equivalent copper neighbors is denoted by $J(AA) = J(BB)$. Type-A coppers have four B-type copper nearest neighbors, two at 5.40 Å (called B_1 in Fig. 6) and the other two at 5.45 Å (called B_2). Type-A coppers are connected to type-B coppers through carboxylate bridges involving an equatorial oxygen of the first copper and an apical oxygen of the second. The path joining a copper type A with coppers type B_1 involves the carboxylate bridge Cu(A)-O(2)-C(1)-O(1)-Cu(B_1), different from the bridge Cu(A)-O(3)-C(4)-O(4)-Cu(B_2) (see Figs. 5 and 6). The magnitude of the exchange interactions between A-B_1 and A-B_2 neighbor copper pairs are denoted $J(AB_1)$ and $J(AB_2)$, respectively. It is important to point out that the difference between $J(AB_1)$ and $J(AB_2)$ is crucial in determining the effective magnetic dimensionality of Cu(L-alanine)$_2$. If $J(AB_1) \approx J(AB_2)$, the spin dynamics would be expected to exhibit a two-dimensional (2D) and nearly isotropic behavior within the copper layer. In the extreme case where $J(AB_1) \gg J(AB_2)$, the copper spins within a layer would be magnetically isolated in "ribbons" parallel to the $\hat{\mathbf{b}}$ axis (see Fig. 6), and the fastest part of the spin dynamics takes place along the ribbons, through the couplings $J(AB_1)$, $J(AA)$, and $J(BB)$.

IV. ANALYSIS OF THE SUSCEPTIBILITY DATA

A. High-temperature behavior

For $T \geq 1.5$ K, the molar susceptibility data for Cu(L-alanine)$_2$ have a Curie-Weiss behavior:

$$\chi_m(T) = \frac{C_m}{T - T_c} . \tag{1}$$

An antiferromagnetic Curie temperature $T_c = -0.70 \pm 0.01$ K, and a Curie constant $C_m = Ng^2\mu_0^2 S(S+1)/3k = 0.426 \pm 0.001$ emu K/mol, were determined by a least-squares fit of the data. Here N is Avodagro's number, g is the g factor averaged over the powder sample, μ_0 is the Bohr magneton, $S = 1/2$ is the effective spin of Cu^{2+} ions, and k is the Boltzmann constant. From the value of C_m, a g factor $g = 2.135 \pm 0.004$ is obtained for the powder sample.

B. Susceptibility data above 0.3 K

The $\chi_m(T)$ versus T data for $T \geq 0.3$ K were analyzed using the Heisenberg model with a Hamiltonian

$$\mathcal{H}_{ex} = -2J \sum_{i=1}^{n} \mathbf{S}_i \cdot \mathbf{S}_{i+1} , \tag{2}$$

where only interactions between nearest-neighbor copper ions are taken into account. The arrangement of the copper ions in the crystal structure of Cu(L-alanine)$_2$ suggests the use of Lines' 2D model for the quadratic layer

antiferromagnet.[15] The exact high-temperature series expansion in powers of $1/T$ yields to[16]

$$\frac{Ng^2\mu_0^2}{\chi_m|J|}=3y+\sum_n \frac{C_n}{y^{n-1}} , \tag{3}$$

where $y=kT/[S(S+1)|J|]$ involves the temperature T and the exchange parameter J. The constants C_n for $n\leq 6$ are tabulated.[15] A least-squares analysis of our data with $0.5<kT/|J|<7$ with Eq. (3) gives $|J|=0.66$ K for the exchange interaction, and $g=2.144$ for the g factor.

We have also analyzed our susceptibility data in terms of the results of Hatfield and collaborators[17] for a uniformly spaced chain of spins $\frac{1}{2}$. These authors followed ideas developed in the classical paper by Bonner and Fisher.[18] However, instead of presenting the results in a tabular form, they reported the algebraic function

$$\chi_m(T)=\frac{Ng^2\mu_0^2}{kT}\frac{\frac{1}{4}+Bx+Cx^2}{1+Dx+Ex^2+Fx^3} , \tag{4}$$

which relates the magnetic susceptibility to $x=|J|/kT$. The values of $B,C,\ldots,F$ are given in Hatfield's paper.[17] Equation (4) reproduces well the results of Ref. 18 for $kT/|J|>0.5$, and provides a method for analyzing susceptibility data with a computer program, instead of using graphical methods. Using Eq. (4) and a least-squares method, we obtained $|J|=0.52$ K, and a g factor $g=2.125$. According to Eq. (2), and to the antiferromagnetic behavior of Cu(L-alanine)$_2$, J has to be negative. The $\chi_m(T)$ versus T curve obtained with Eq. (4) and $|J|=0.52$ K is displayed in Fig. 1. The $\chi_m(T)$ versus T curves calculated with Eqs. (3) and (4), shown together in Fig. 2, indicate that the agreement of the data with a one-dimensional (1D) spin chain model is better at low temperatures than that with a 2D quadratic layer antiferromagnet. It is worthwhile to point out that, since the susceptibility data were obtained in a powder sample, the information about its angular variation is lost. An angular dependence of the susceptibility would be expected for Cu(L-alanine)^2 because of the anisotropy of $g^2(\theta,\Phi)$. However, according to Eqs. (3) and (4), this g anisotropy would not change the shape of the temperature variation of the susceptibility as 1D or 2D behavior do, but only add a multiplicative factor in the $\chi_m(T)$ curve (the average value of g^2).

Anisotropic contributions to the exchange and dipole-dipole interactions could give rise to differences in the shape of $\chi_m(T)$ from those predicted by the model systems [Eqs. (3) and (4)]. These contributions have not been evaluated, and are thought to contribute at temperatures lower than those that determine the 1D or 2D behavior for $\chi_m(T)$ in Fig. 2. Thus, within the simplicity of the calculations, our susceptibility data support a 1D antiferromagnetic spin chain model, instead of the 2D behavior suggested by the crystal structure of Cu(L-alanine)^2.

The 1D behavior may be understood considering the results of Levstein and Calvo[7] (see also Ref. 8), who analyzed values of the exchange parameters $J(AB)$, obtained in three similar Cu(aa)$_2$ using the same experimental method, in terms of the structural information. They found that the main contribution arises from the carboxylate bridges connecting these A and B ions. As discussed in Sec. III, the structure of these carboxylate groups, and the distance between the copper ion and the equatorial oxygen ligands, are fairly constant along the different Cu(aa)$_2$. Then, the values of $J(AB)$ depend mainly on the distance d(Cu-O$_{Ap}$) between the copper and the apical oxygen ligands. Since these distances [d(Cu-O(2''))=2.70 Å and d(Cu-O(4'))=2.90 Å] are very different for Cu(L-alanine)$_2$, we may expect a much larger efficiency of the superexchange paths provided by the carboxylate groups involving C(1), O(1), and O(2) than for those involving C(4), O(3), and O(4) (see Figs. 5 and 6). This may result in a preferred direction along $\hat{\mathbf{b}}$ for the spin dynamics, and the spin excitations would travel mainly through "ribbons" parallel to $\hat{\mathbf{b}}$ as those shaded in Fig. 6.

C. Susceptibility data below 0.3 K

The susceptibility data below 0.3 K show a complex T dependence with a rounded peak and a depression. Changes in $\chi_m(T)$ in this range can result from details of the exchange network. The low symmetry of Cu(L-alanine)$_2$ complicates the analysis of the problem, as several different exchange parameters have to be considered. We do not have a detailed explanation for the behavior of $\chi_m(T)$ below 0.3 K. We mention, however, possible contributions to the observed $\chi_m(T)$.

For most orientations of the applied magnetic field, the g factors for copper ions in lattice sites A and B are different. This may result in measurable changes of $\chi_m(T)$ at temperatures lower than that corresponding to the susceptibility maximum. Also, if $J(AB_1)$ is the most important interaction, the terms characterized by $J(AA)$ and $J(BB)$ coupling AA and BB nearest-neighbor copper pairs in the spin chain (not considered in Hatfield's model[17]) could contribute to the behavior of $\chi_m(T)$ at low T. In addition, lattice defects may leave some short spin chains with an odd number of spins. These chains could behave as a paramagnet, and produce the increase of $\chi_m(T)$ at very low T.

The hyperfine interactions in Cu(aa)$_2$ have magnitudes equivalent to magnetic fields of 20–200 G (normal for Cu^{2+}). These internal fields may be responsible for the minimum of $\chi_m(T)$ observed at 0.035 K.[19]

V. ANALYSIS OF THE EPR DATA

A. The magnetic interactions

The magnetic moment corresponding to a spin system made of two species $\mathbf{S}_{iA}$ and $\mathbf{S}_{iB}$ of copper spins can be written as

$$\mathbf{M}=-\mu_0\sum_i(\mathsf{g}_A\cdot\mathbf{S}_{iA}+\mathsf{g}_B\cdot\mathbf{S}_{iB})=-\mu_0(\mathsf{g}\cdot\mathbf{S}+\mathsf{G}\cdot\mathbf{s}) , \tag{5}$$

where g_A and g_B are the g tensors of spins in sites A and B, and

$$\mathsf{g}=\tfrac{1}{2}(\mathsf{g}_A+\mathsf{g}_B),\quad \mathsf{G}=\tfrac{1}{2}(\mathsf{g}_A-\mathsf{g}_B) , \tag{6a}$$

$$\mathbf{S}=\sum_i\mathbf{S}_{iA}+\sum_i\mathbf{S}_{iB}=\mathbf{S}_a+\mathbf{S}_B,\quad \mathbf{s}=\mathbf{S}_A-\mathbf{S}_B . \tag{6b}$$

In Eqs. (5) and (6b), **S** is the total spin and the sums are over the unit cells of the crystal. The effective Hamiltonian describing this system in a field **H** is

$$\mathcal{H}=\mathcal{H}_z+\mathcal{H}_{\rm ex}+\mathcal{H}_{dd}+\mathcal{H}'' , \tag{7}$$

where $\mathcal{H}_z$, $\mathcal{H}_{\rm ex}$, and $\mathcal{H}_{dd}$ are, respectively, the Zeeman, exchange, and dipole-dipole contributions to the Hamiltonian. The contribution $\mathcal{H}''$ to Eq. (7) involves other interactions, as hyperfine couplings, anisotropic and antisymmetric exchange interactions, etc. These terms are less important for our purpose, and will not be analyzed in detail.

Considering Eq. (5), the Zeeman Hamiltonian,

$$\mathcal{H}_z=-\mathbf{M}\cdot\mathbf{H}=\mu_0\mathbf{H}\cdot\mathsf{g}\cdot\mathbf{S}+\mu_0\mathbf{H}\cdot\mathsf{G}\cdot\mathbf{s}=\mathcal{H}_z^0+\mathcal{H}_z' , \tag{8}$$

is divided in two components, $\mathcal{H}_z^0$ and $\mathcal{H}_z'$, where $\mathcal{H}_z^0$ is proportional to the total spin **S**, while $\mathcal{H}_z'$ is proportional to the G tensor defined in Eq. (6a). The exchange coupling $\mathcal{H}_{\rm ex}$ in Eq. (7) is assumed to be isotropic, as in Eq. (2).

To pursue this further, a perturbative calculation is usually adopted, and the Hamiltonian $\mathcal{H}$ of Eq. (7) is divided as

$$\mathcal{H}=\mathcal{H}_0+\mathcal{H}' , \tag{9a}$$

with

$$\mathcal{H}_0=\mathcal{H}_z^0+\mathcal{H}_{\rm ex} , \tag{9b}$$

$$\mathcal{H}'=\sum_i\mathcal{H}_i'=\mathcal{H}_z'+\mathcal{H}_{dd}+\mathcal{H}'' , \tag{9c}$$

where $\mathcal{H}_0\gg\mathcal{H}'$ for Cu(L-alanine)$_2$. Since $\mathcal{H}_z^0$ is proportional to S_z, $\mathcal{H}_z^0$ commutes with $\mathcal{H}_{\rm ex}$, and the EPR spectrum is a single line with the g tensor defined in Eq. (6a) as the average of g_A and G_B. The contributions of $\mathcal{H}'$ of Eq. (9c) are modulated by $\mathcal{H}_0$ and, in a zeroth-order approach valid for $\mathcal{H}_0\gg\mathcal{H}'$, they are averaged to zero.[20,21] In this case the detailed information concerning the difference G between g_A and g_B, the dipole-dipole interaction $\mathcal{H}_{dd}$, and any other term contained in $\mathcal{H}'$, is lost.

B. The g tensor

The collective resonance of the copper spins in the lattice coupled by the exchange interaction is described by the spin Hamiltonian,

$$\mathcal{H}_s=\mu_0\mathbf{H}\cdot\mathsf{g}\cdot\mathbf{S} , \tag{10}$$

where g is defined in Eq. (6a). The squared g factor $g^2(\theta,\Phi)=\hat{\mathbf{h}}\cdot\mathsf{g}\cdot\mathsf{g}\cdot\hat{\mathbf{h}}$, measured for **H** applied along $\hat{\mathbf{h}}=\mathbf{H}/|\mathbf{H}|=(\sin\theta\cos\Phi,\sin\theta\sin\Phi,\cos\theta)$ in the xyz system, was evaluated from the position in magnetic field at resonance, and the microwave frequency. The components of $\mathsf{g}^2=\mathsf{g}\cdot\mathsf{g}$ obtained from the data at 9 and 35 GHz are given in Table I and were used to obtain the plots in Fig. 3.

For small anisotropies it is

$$\mathsf{g}^2=\tfrac{1}{2}(\mathsf{g}_A^2+\mathsf{g}_B^2) . \tag{11}$$

TABLE I. Components $(g^2)_{ij}$ of the squared gyromagnetic tensor obtained by least-squares fits of the function $g^2(\theta,\Phi)=\hat{\mathbf{h}}\cdot\mathsf{g}\cdot\mathsf{g}\cdot\hat{\mathbf{h}}$ where $\hat{\mathbf{h}}=\mathbf{H}/|\mathbf{H}|$ is the direction of the applied field, to the data at 9 and 35 GHz. The components $(g^2)_{xy}$ and $(g^2)_{zy}$ are zero by symmetry conditions. The eigenvalues of this tensor are indicated by $(g^2)_1$, $(g^2)_2$, and $(g^2)_3$, and are included in the table. The uncertainties given in parentheses were obtained from the dispersion of the data. The values of $g_\parallel$ and $g_\perp$ were calculated assuming axial symmetry for the molecular gyromagnetic tensors of copper ions on sites A and B. The angle 2α between the symmetry axes of these sites and their orientations (θ_m,Φ_m) in the coordinate system $(xyz)=(a'bc)$ calculated from the EPR data at each frequency are included. These angles and orientations should be compared to those calculated from the structural data (Sec. III).

ν (GHz)	35	9
$(g^2)_{xx}$	4.626(1)	4.598(1)
$(g^2)_{yy}$	4.436(1)	4.396(1)
$(g^2)_{zz}$	4.464(1)	4.481(1)
$(g^2)_{zx}$	0.310(1)	0.333(1)
$(g^2)_1$	4.865(1)	4.878(1)
$(g^2)_2$	4.225(1)	4.201(1)
$(g^2)_3$	4.437(1)	4.396(1)
$g_\parallel$	2.253	2.253
$g_\perp$	2.055	2.050
2α	120.2	124.0
(θ_m,Φ_m)	(58.0,36.0)	(55.5,35.0)

The principal components of g_A^2 and g_B^2 are calculated from those of g^2 using Eq. (11), and assuming axial symmetry, as suggested by the crystallographic data for Cu(L-alanine)$_2$. Following Refs. 22 and 23, and according to Ref. 2, we obtained $g_\parallel$ and $g_\perp$ for the molecular g tensor and (θ_m,Φ_m) for the direction where $g_\parallel$ would be measured for each lattice site, 2α being the angle between these two directions (see Table I). These values of (θ_m,Φ_m) and 2α are in good agreement with those obtained from the crystallographic data, indicating that the assumption of axial symmetry is valid. The values of $g_\parallel$ and $g_\perp$ are similar to those observed for copper impurities in L-alanine single crystals,[24] supporting a $d(x^2-y^2)$ ground orbital state, sited on the plane of the N_2O_2 set of equatorial ligands to copper.

C. EPR linewidths

Anderson's[20] and Kubo and Tomita's[21] exchange-narrowing theories use stochastic methods and a second-order perturbation calculation to analyze the effect of $\mathcal{H}'$ on the EPR linewidths. In these models, each term $\mathcal{H}_i'$ of $\mathcal{H}'$ [Eq. (9c)] gives rise to a contribution ΔH_i to the linewidth of the resonance which in field units is given by

$$\Delta H_i=(M_i^2/g\mu_0\hbar)/\omega_{\rm ex}^i , \tag{12}$$

where M_i^2 is the second moment of $\mathcal{H}_i$, and $\omega_{\rm ex}$ is a characteristic modulation frequency associated to $\mathcal{H}_i'$, and produced by $\mathcal{H}_{\rm ex}$ because $\mathcal{H}_i'$ and $\mathcal{H}_{\rm ex}$ do not commute. Equation (12) is valid for secular interactions,

commuting with $\mathcal{H}_z^0$, which are not modulated at the Larmor frequency, and when $\hbar\omega_{ex} \gg (M_i^2)^{1/2}$. Then, in the presence of exchange, ΔH_i is a factor $(M_i^2)^{1/2}/\hbar\omega_{ex}$ smaller than the linewidth $(M_i^2)^{1/2} g\mu_0$, measured in the absence of exchange.

The effect on the linewidth introduced by $\mathcal{H}_z'$ of Eq. (8) has been analyzed by Yokota and Koide[25] and by Levstein *et al.*,[4] who obtained

$$\Delta H_z(\theta,\Phi) = \frac{(2\pi/3)^{1/2}[g_A(\theta,\Phi) - g_B(\theta,\Phi)]^2 \omega_0^2 \hbar}{4g^3(\theta,\Phi)\omega_{ex}\mu_0} , \quad (13)$$

which increases with the square of the microwave frequency ω_0 of the experiment.

Richards and Salamon[26] proved that Eq. (12) is not valid in systems of low magnetic dimensionality. Since the spin dynamics is diffusive at long times, and diffusion is slow in 1D and 2D, Eq. (12) is valid only in three dimensions. This is important for interactions bilineal in spin operators, like dipole dipole, for which Eq. (12) gives a wrong angular dependence of the linewidth. For a 2D lattice, Richards and Salamon[26] (see also Ref. 6) predict a dipole-dipole contribution to the linewidth given by

$$\Delta H_{dd} = A_{dd}[\text{const} + (3\cos^2\theta_n - 1)^2] , \quad (14)$$

where θ_n is the angle between **H** and the normal to the plane of coppers. Equation (14) was obtained for the cases where the exchange network (which depends on the chemical paths connecting the magnetic ions) and the dipolar interactions (which depend only on the distances between the spins) have both 2D characteristics.

It has to be stressed that Eqs. (13) and (14) give contributions to the linewidth with angular dependences including fourth-order spherical harmonics. Hyperfine interactions and the antisymmetric contribution to the exchange interaction contained in $\mathcal{H}$ of Eq. (9c) introduce contributions transforming like second-order spherical harmonics.[4] Other terms of $\mathcal{H}'$ of Eq. (9c) giving forth-order contributions to the linewidth seem to be small for Cu(L-alanine)$_2$, and we assume that the observed peak-to-peak linewidth ΔH_{pp} is the sum of Eqs. (13) and (14), plus the four terms having second-order angular dependences allowed by the crystal symmetry of Cu(L-alanine)$_2$. Then, ΔH_{pp} is compared to the function

$$\begin{aligned}\Delta H_{pp} = {} & A_1\sin^2\theta\cos^2\Phi + A_2\sin^2\theta\sin^2\Phi + A_3\cos^2\theta \\ & + 2A_4\sin\theta\cos\theta\cos\Phi \\ & + A_5[g_A(\theta,\Phi) - g_B(\theta,\Phi)]^2 \\ & + A_6(3\sin^2\theta\cos^2\Phi - 1)^2 , \end{aligned} \quad (15)$$

where θ and Φ give the orientation of the applied magnetic field in the $xyz \equiv a'bc$ coordinate system. The fifth term in Eq. (15) corresponds to Eq. (13) and then[4]

$$A_5 = \frac{(2\pi/3)^{1/2}\omega_0^2\hbar}{4g^3\omega_{ex}\mu_0} , \quad (16)$$

where g is the average of the g tensor. The sixth term of Eq. (15) corresponds to Eq. (14) in the xyz coordinate system. The values of the parameters A_i of Eq. (15) were obtained by a least-squares calculation from the linewidth data included in Fig. 4. They are given in Table II for the two microwave frequencies, and the lines shown in Fig. 4 are obtained with these values.

TABLE II. Values of the parameters A_i (in G) obtained by fitting EQ. (15) to the experimental values of the linewidth measured at 35 and 9 GHz, displayed in Fig. 6. The uncertainties of these values were obtained from the dispersions of the fits.

ν (GHz)	35	9
A_1	90.0±2.5	108±1
A_2	44.6±1.4	100±1
A_3	40±1	77.6±0.5
A_4	13±1	3±1
A_5	2365±100	−400±100
A_6	20±1	14.1±0.3

The magnitudes of the coefficients $A_1 - A_4$ are a consequence of hyperfine interactions and antisymmetric and anisotropic exchange; they are not important for our purpose, and are not analyzed in detail. Their dependence with the microwave frequency can be related to nonsecular contributions to the linewidth, which produce smaller values of A_1, A_2, and A_3 of Eq. (15) at the higher frequency. At 9.2 GHz, A_4 is close to zero.

The fifth contribution to Eq. (15) contains fourth-order angular functions, but also some second-order contributions. It is not strictly orthogonal to the first (second-order) functions involving $A_1 - A_4$, in the range of field orientations covered by our experiments. This fact introduces an uncertainty on the determination of the coefficient A_5 by the least-squares procedure, which is not considered in the uncertainties given in Table II (obtained from the dispersion of the fit). Although the contribution to the linewidth of the value $A_5 = -400 \pm 100$ G obtained at X band is small (maximum of 6±1.5 G, compared with contributions of up to 100 G of the other terms), its negative sign is somewhat stunning. It could be due to nonsecular terms of the antisymmetric exchange, as well as to antisymmetric terms arising from the dipole-dipole interaction between nonequivalent anisotropic spins.[27] The nonorthogonality of the functions included in the fit [Eq. (15)] could also contribute to the negative value. In view of the small magnitude of this contribution at X band, we have not attempted a detailed evaluation of other mechanisms contributing to A_5.

The magnitude of the coefficient A_5 greatly increases at 35 GHz, as expected by Eq. (16), and the value given in Table II allows one to calculate $\omega_{ex} = (2\pi)13.95$ GHz as the exchange frequency related to H_z'. Considering that,[4]

$$\omega_{ex}^2 = 4S(S+1)\{Z_1[J(AB_1)]^2 + Z_2[J(AB_2)]^2\}/3\hbar^2 ,$$

where Z_1 and Z_2 are the number of nearest neighbors type B_1 and B_2 to a copper type A. Assuming $Z_1 = Z_2 = 2$ and $J(AB_1) = J(AB_2) = J(AB)$ (i.e., four equivalent B-type copper neighbors), it is found that

$$|J(AB)| = 0.33 \text{ K} .$$

If, instead, $J(AB_2) \ll J(AB_1)$ is assumed, then $Z_1 = 2$

and $Z_2=0$ [or $J(AB_2)\approx 0$], i.e., only two copper neighbors contribute, it is found that

$$|J(AB_1)|=0.47 \text{ K} .$$

These values will be discussed in the next section and compared with that obtained from the susceptibility data.

The contribution of the sixth term of Eq. (15) is large at both 9.2 and 35 GHz, indicating a low-dimensional behavior of the spin dynamics of Cu(L-alanine)$_2$.[6,26] Besides using the function proposed by Richards and Salamon[26] for the angular variation of the linewidth of spin systems with a 2D spin dynamics [Eq. (14)], as one of the contributions to Eqs. (15), an attempt was made to improve the fit by using instead

$$\Delta H_{dd} \propto [(3\cos^2\theta_n-1)-3\sin^2\theta_n\cos(2\Phi_n)]^2 . \quad (17)$$

As shown in the Appendix, Eq. (17) can be derived from the secular part of the dipolar interaction for an array of magnetic ions in a square planar lattice, assuming a spin dynamics predominantly oriented along the $\hat{\mathbf{b}}\equiv\hat{\mathbf{y}}$ axis, with weaker exchange links along the $\hat{\mathbf{c}}=\hat{\mathbf{z}}$ axis. In Eq. (17) θ_n and Φ_n are measured in a system where the $\hat{\mathbf{x}}$ axis is along the normal to the bc plane of the copper layers. This attempt was performed in order to verify whether the tendency to a 1D behavior suggested by the susceptibility data is also reflected by the spin dynamics, through the angular variation of the linewidth. However, the quality of the fit deteriorates substantially when Eq. (17) replaces Eq. (14) as the last term of Eq. (15). This indicates that we are not in the limit where the exchange parameter J connecting copper chains along the $\hat{\mathbf{b}}$ axis (see Fig. 6) is much larger than the exchange coupling connecting neighboring chains.

From the structural data it would not be correct to assume for Cu(L-alanine)$_2$ that the dipolar interaction is mainly of 1D nature and also that the intrachain exchange interaction is much larger than the interchain interaction, as in the system studied by Hennessy *et al.*[28] As shown by these authors this would have led to the function $(3\cos^2\theta-1)^2$, with θ measured from the chain axis, and a Lorentzian line shape. Then, we conclude that the linewidth data indicate a 2D spin dynamics, with layers in the zy plane, giving rise to EPR linewidths which follow the theory of Richards and Salamon.[26]

VI. CONCLUSIONS

Our magnetization measurements in Cu(L-alanine)$_2$ cover a wide range of temperatures; the rounded peak in the susceptibility data at 0.67 K suggests a low-dimensional magnetic behavior.[14] The data above 0.3 K favor a 1D spin chain, with $J=-0.52$ K.

The g tensor and the EPR linewidth have been measured at room temperature, at 9 and 35 GHz. The values obtained at 9 GHz agree will with those reported earlier by Yokoi and Ohsawa.[13] The g tensor reflects a $d(x^2-y^2)$ ground-state orbital and the orientations of the two crystal sits for copper in Cu(L-alanine)$_2$. The averaged g factor obtained from the susceptibility data in the Curie-Weiss regime also agrees with the average of the g tensor obtained from the EPR data.

The angular variation of the linewidth was analyzed. An important contribution observed at 35 GHz is attributed to a residual Zeeman term, which takes into account the difference between the gyromagnetic tensors of the copper ions at the two different lattice sites [$\mathcal{H}'_z$ of Eq. (8)]. From this frequency-dependent term we extract an exchange frequency related to $\mathcal{H}'_z$, which allows calculation of the exchange coupling parameters between nonequivalent A-B neighbor copper spin pairs. When it is assumed that each type-A copper interacts with only two of those copper (B_1) neighbors (as in a 1D spin chain), the model gives $|J(AB_1)|=0.47$ K.

The values $|J|=0.52$ K, obtained from the susceptibility data, and $|J(AB_1)|=0.47$ K, obtained from the linewidth data assuming that each type-A copper interacts only with two type-B copper neighbors (called B_1), are very similar. This suggests that $J\approx J(AB_1)$, and the exchange interactions in the "ribbon" spin chains of Fig. 6 are essentially those between a type-A copper and the two closest type-B copper ions, introducing $J(AA)=J(BB)$ smaller contributions. This indicates that the carboxylate bridges connecting AB_1 copper pairs are more efficient superchange paths than the hydrogen bonds bridging AA or BB copper neighbors.

Another important contribution to the linewidth has the angular variation predicted by the theory of Richards and Salamon[26] [Eq. (14)] for the exchange-narrowed dipole-dipole interaction in a 2D exchange network. A 2D magnetic behavior may be expected for Cu(L-alanine)$_2$ in view of its layered crystal structure (see Ref. 12 and Sec. III of this paper).

To conciliate the discrepancy between the different magnetic dimensionalities which result from our modeling of the susceptibility and the contributions to the EPR linewidth, we should point out that the models used for both the susceptibility and the exchange narrowing of the EPR signal give only a tendency for the magnetic dimensionality of the spin system. The changes in the predictions of the theory by Richards and Salamon[26] when the exchange network is not clearly 2D may be understood along the work of Hennessy *et al.*[28] They analyze the deviations from ideal 1D behavior when weak interchain and interlayer exchange coupling are not negligible. In fact, the Lorentzian line shapes observed in our experiments give an indication that they are not negligible in Cu(L-alanine)$_2$.

In Sec. III we examine the role as superexchange paths between copper ions in Cu(L-alanine)$_2$ played by the carboxyl bridges, using the crystallographic data. There, we suggest that the difference between the structure of the carboxyl bridges connecting nonequivalent copper ions can split off magnetically the copper layers of Cu(L-alanine)$_2$ in 1D magnetic ribbons. We can now estimate the magnitude of the exchange coupling $J(AB_2)$ between ribbons. Assuming that $|J(AB_1)|=0.47$ K, obtained from the contribution of Eq. (13) to the linewidth, corresponds to the intraribbon exchange, we can estimate $J(AB_2)$ (see Fig. 6) on the grounds of the work of Levstein and Calvo[7] (see also Ref. 8), who correlate the variation of the exchange constant with the Cu-O_{ap} distance,

in a series of similar carboxylate-bridged $Cu(aa)_2$. This correlation gives a straight line with a slope $\delta|J|/\delta d(\text{Cu-O}_{ap}) \approx -2.7$ K/Å. The absolute magnitude of the exchange as a function of $d(CuO_{ap})$ may change between compounds which are not similar to those considered in Ref. 7. However, the ratio $\delta|J|/\delta d(\text{Cu-O}_{ap})$ is assumed to be approximately valid for other carboxylate-bridged $Cu(aa)_2$. Since $|J(AB_1)|=0.47$ K corresponds to $d(\text{Cu-O}_{ap})=2.7$ Å (see Fig. 5), one can estimate that for $d(\text{Cu-O}_{ap})=2.9$ Å it is $|J(AB_1)|/|J(AB_2)| \approx 9$. From this value we can calculate the characteristic time t_0 in which the 1D diffusive spin polarization starts making transitions and relaxes off the linear chain. According to Hennesy *et al.*,[28] who use the relationship between J and the 1D diffusion constant, and, as given by Tahir-Kheli and McFadden,[29] the value of t_0 is

$$t_0=(3\sqrt{2}/8)^{2/3}\sqrt{\pi}[J(AB_1)/J(AB_2)]^{1/3}\hbar/J(AB_2), \tag{18}$$

which gives $t_0 \approx 3.5\times10^{-10}$ sec, corresponding to about 1000 G in field units, for $g \approx 2$. It is to be noted that this is a very crude approximation since for $|J(AB_1)/J(AB_2)| \approx 9$ the validity of the perturbative calculation performed by Hennesy *et al.*[28] to derive Eq. (18) cannot be guaranteed. However, this provides us with a 2D diffusive process.

Considering that the EPR linewidths of $Cu(\text{L-alanine})_2$ are in the order of 150 G ($\delta t \approx 2.4\times10^{-9}$ sec), the measuring time is almost one order of magnitude longer than t_0, indicating that we would be in the regime where the 1D process has already switched into 2D (anisotropic) diffusion. This may explain why the angular variation of the linewidth reflects a 2D behavior of the spin dynamics. From the ratio $|J(AB_1)/J(AB_2)| \approx 9$ estimated above, we can also understand the tendency to a 1D behavior observed in the susceptibility data about 0.3 K, although measurements of the susceptibility in single-crystal samples would be required in order to gain additional insight in this matter.

Our interpretation of the linewidth data is different from that of Yokoi and Ohsawa.[13] They used the theory of Anderson[20] without considering the effect of the magnetic dimensionality, described later by Richards and Salamon,[28] being then unable to describe the observed angular variation of ΔH. Furthermore, since their experiments were performed at 9 GHz, the contribution of the fifth term of our Eq. (15) was not observed by these authors.[13]

After this paper was completed, we learned of recent results of Wakamatsu *et al.*,[30] who reported specific heat measurements in the copper salt of the amino acid L-isoleucine, in the very low-T range. Previous magnetic susceptibility data on $Cu(\text{L-isoleucine})_2\cdot H_2O$ obtained by Newman *et al.*[1] had shown a transition to a ferromagnetic phase at 0.117 K, and suggested a dominant 2D magnetic behavior at higher T. This 2D behavior is expected in view of the layered arrangement of copper ions in the crystal lattice of $Cu(\text{L-isoleucine})_2\cdot H_2O$.[31] Considering their measurements of the angular variation of the EPR linewidth, and the particular way in which the resonances arising from the four nonequivalent copper ions in the unit cell collapse by pairs, Calvo *et al.*[32] also proposed a 2D magnetic behavior for $Cu(\text{L-isoleucine})_2\cdot H_2O$. Surprisingly, the specific heat data of Wakamatsu *et al.*[30] above the transition temperature can be interpreted in terms of a 1D spin system, instead of a 2D one. These authors[30] claim for $Cu(\text{L-isoleucine})_2\cdot H_2O$, as we do here for $Cu(\text{L-alanine})_2$, a magnetic splitting of the copper layers in zigzag chains along a crystal axis. The superexchange paths between coppers in $Cu(\text{L-isoleucine})_2\cdot H_2O$ seem to be hydrogen bridges [instead of carboxyl groups, as in $Cu(\text{L-alanine})_2$]. Then, the splitting is produced by the differences between hydrogen bridges connecting coppers within a particular layer. A quantitative analysis of the specific heat data is not performed by these authors.[30]

ACKNOWLEDGMENTS

This work was supported by Grants from Consejo Nacional de Investigaciones Científicas y Tecnicas (CONICET), Argentina, Conselho Nacional de Pesquisa (CNPq), Financiadora de Estudos e Projetos (FINEP), and Fundação de Amparo à Pesquisa do Estado de São Paulo (FAPESP) of Brasil. The authors are grateful to P. R. Levstein for her collaboration in the analysis of the data, to C. A. Steren for the crystallographic figures, and to M. A. Mesa for assistance with some of the experimental work.

APPENDIX

The decay of the transverse magnetization can be described in terms of the relaxation function $\Phi(t)$ which is approximated by[21]

$$\Phi(t)=\exp\left[-\int_0^t (t-\tau)\phi(\tau)d\tau\right], \tag{A1}$$

where

$$\phi(\tau)=\frac{\hbar^{-2}\langle[\mathcal{H}'(\tau),S_+][S_-,\mathcal{H}']\rangle}{\langle S_+S_-\rangle}$$

with

$$\mathcal{H}'(\tau)=\exp(i\mathcal{H}_{ex}\tau/\hbar)\mathcal{H}'\exp(-i\mathcal{H}_{ex}\tau/\hbar),$$

and $\mathcal{H}'$ is defined in Eq. (9c) and $\mathcal{H}_{ex}$ is the exchange Hamiltonian defined in Eq. (2).

The line profile at a frequency ω is then proportional to

$$I(\omega)=\int_{-\infty}^{\infty}\Phi(t)\exp[i(\omega-\omega_0)t]dt, \tag{A2}$$

where ω_0 is the resonance frequency. If it is assumed that the main source of broadening comes from the secular part of the dipolar interaction, $\phi(\tau)\approx\phi_d(\tau)$, where the dipolar contribution $\phi_d(\tau)$ is given by[28]

$$\phi_d(\tau)=9g^4\mu_0^4N^{-1}\sum_{\mathbf{q}}|F_{\mathbf{q}}|^2\langle S_{\mathbf{q}}^{\hat{\mathbf{h}}}(\tau)S_{-\mathbf{q}}^{\hat{\mathbf{h}}}\rangle^2, \tag{A3}$$

where[6]

$$\langle S_{\mathbf{q}}^{\hat{\mathbf{h}}}(\tau)S_{-\mathbf{q}}^{\hat{\mathbf{h}}}\rangle=N^{-1}\sum_{i,j}\langle S_i^{\hat{\mathbf{h}}}(\tau)S_j^{\hat{\mathbf{h}}}\rangle\exp(i\mathbf{q}\cdot\mathbf{R}_{ij})$$

and

$$F_{\mathbf{q}}=\sum_{i,j}R_{ij}^{-3}[1-3(\hat{h}\cdot\mathbf{R}_{ij})^2]\exp(-i\mathbf{q}\cdot\mathbf{R}_{ij}).$$

In Eq. (A3) the sum is over the first Brillouin zone, $\langle S^{\hat{\mathbf{h}}}_{\mathbf{q}}(\tau)S^{\hat{\mathbf{h}}}_{-\mathbf{q}}\rangle$ are the correlation functions, and $\hat{\mathbf{h}}$ is the direction of the applied magnetic field. Equation (A3) shows that the angular dependences for each $\mathbf{q}$ component are contained in the $|F_{\mathbf{q}}|^2$, and these are weighted by the correlation functions to give $\Phi(t)$ using Eq. (A1). Note that these "weighting factors" depend on time, and it is only as $\tau\rightarrow 0$ that the angular variation tends to that given by the second moment, proportional to $\sum_{\mathbf{q}}|F_{\mathbf{q}}|^2$.

Let us consider now a 2D lattice with a square planar configuration. In the diffusive regime the process takes place along the two perpendicular coordinate axes, and

$$\langle S^{\hat{\mathbf{h}}}_{\mathbf{q}}(\tau)S^{\hat{\mathbf{h}}}_{-\mathbf{q}}\rangle \approx [S(S+1)/3]\exp[-(D_y q_y^2 + D_z q_z^2)\tau] , \tag{A4}$$

where D_y and D_z are diffusion constants along $\hat{\mathbf{y}}$ and $\hat{\mathbf{z}}$. In that case, for very long times, the angular variation is dominated by $|F_{\mathbf{q}=0}|^2$ because of the filtering effect of the Gaussian functions in q_y and q_z when Eq. (A4) is replaced in Eq. (A3). If diffusion occurs preferentially along one direction (say $\hat{\mathbf{y}}$), with only weak exchange links along $\hat{\mathbf{z}}$, allowing spin relaxation off the chains, we may write, according to Hennessy *et al.*[28]

$$\langle S^{\hat{\mathbf{h}}}_{\mathbf{q}}(\tau)S^{\hat{\mathbf{h}}}_{-\mathbf{q}}\rangle \approx [S(S+1)/3]\exp(-D_y q_y^2\tau)\tilde{\Phi}_{qz}(\tau) ,$$

where $\tilde{\Phi}_{qz}(\tau)$ describes the departure from the one-dimensional diffusive process. If we assume $D_z=0$, it is $\tilde{\Phi}_{qz}(\tau)\approx 1$ (no relaxation off the chain), the angular variation will be determined by

$$\sum_{q_z} |F_{q_y=0,q_z}|^2 .$$

In a square planar lattice with parameter a, it is

$$\mathbf{R}_j = a(m\hat{\mathbf{e}}_y + n\hat{\mathbf{e}}_z) ,$$

where m and n are integers, not simultaneously zero. In this coordinate system, where $\hat{\mathbf{e}}_x$ is perpendicular to the copper layers, it has been shown that[26]

$$|F_{\mathbf{q}=0}|^2 \propto (3\cos^2\theta - 1)^2$$

while

$$\sum_{q_z} |F_{q_y=0,q_z}|^2 \propto [(3\cos^2\theta - 1) - 3\sin^2\theta\cos(2\Phi)]^2$$

when the spin dynamics occurs mainly along the $\hat{\mathbf{y}}=\hat{\mathbf{b}}$ axis. It is worthwhile to remember that

$$\sum_{\mathbf{q}} |F_{\mathbf{q}}|^2 \propto (3\cos^2\theta - 1)^2 + 9\sin^4\theta\cos^2(2\Phi)$$

is obtained for the second moment of the dipolar interaction of a 3D magnetic system. In the last three equations θ and Φ give the orientation of the applied magnetic field in the system of coordinates where the copper layers are in the zy plane, and $\hat{\mathbf{x}}$ is the normal to the layers.

[1] P. R. Newman, J. L. Imes, and J. A. Cowen, Phys. Rev. B **13**, 4093 (1976).
[2] R. Calvo and M. A. Mesa, Phys. Rev. B **28**, 1244 (1983).
[3] R. Calvo, M. A. Mesa, G. Oliva, J. Zukerman-Schpector, O. R. Nascimento, M. Tovar, and R. Arce, J. Chem. Phys. **81**, 4584 (1984).
[4] P. R. Levstein, C. A. Steren, A. M. Gennaro, and R. Calvo, Chem. Phys. **120**, 449 (1988).
[5] S. K. Hoffmann, J. Gozlar, and L. S. Sczepaniak, Phys. Rev. B **37**, 7331 (1988).
[6] P. M. Richards, in *Local Properties at Phase Transitions,* International School of Physics, Enrico Fermi, Course LIX-Varenne on Lake Como, 1973, edited by K. D. Mueller and A. Rigemonti (North-Holland/Elsevier, Amsterdam, 1976).
[7] P. R. Levstein and R. Calvo, Inorg, Chem. **29**, 1581 (1990).
[8] P. R. Levstein, R. Calvo, E. E. Castellano, O. E. Piro, and B. E. Rivero, Inorg. Chem. **29**, 3918 (1990).
[9] R. Calvo, and M. C. G. Passeggi, R. A. Isaacson, M. Y. Okamura, and G. Feher, Biophys. J. **58**, 149 (1990).
[10] R. Calvo and M. A. Mesa, Bull. Am. Phys. Soc. **28**, 256 (1983).
[11] R. Calvo and M. A. Novak, S. B. Oseroff, and O. G. Symko, in *Proceedings of the 18th International Conference in Low Temperature Physics, Kyoto, 1987* [Jpn. J. Appl. Phys. **26**, Suppl. **3**, 861 (1987)].
[12] A. Dijkstra, Acta Ctystallogr. **20**, 588 (1966).
[13] H. Yokoi and H. Ohsawa, Bull. Chem. Soc. Jpn. **46**, 2766 (1973).
[14] L. J. de Jongh and A. R. Miedema, Adv. Phys. **23**, 1 (1974).
[15] M. E. Lines, J. Phys. Chem. Solids **31**, 101 (1970).
[16] G. S. Rushbrooke and P. J. Woods, Mol. Phys. **1**, 257 (1958).
[17] J. W. Hall, Ph. D. dissertation, University of North Carolina, Chapel Hill, 1977; W. E. Hatfield, J. Appl. Phys. **52**, 1985 (1981).
[18] J. C. Bonner and M. E. Fisher, Phys. Rev. A **135**, 640 (1964).
[19] J. L. Imes, G. L. Neiheisel, and W. P. Pratt, Phys. Lett. **49A**, 351 (1974).
[20] P. W. Anderson and P. R. Weiss, Rev. Mod. Phys. **25**, 269 (1953); P. W. Anderson, J. Phys. Soc. Jpn. **9**, 316 (1954).
[21] R. Kubo and K. Tomita, J. Phys. Soc. Jpn. **9**, 888 (1954).
[22] H. Abe and K. Ono, J. Phys. Soc. Jpn. **11**, 947 (1956).
[23] D. E. Billing and B. J. Hathaway, J. Chem. Phys. **50**, 1476 (1969).
[24] K. Takeda, Y. Arata, and S. Fujiwara, J. Chem. Phys. **53**, 854 (1970); M. Fujimoto and J. Janecka, *ibid.* **55**, 1152 (1971); M. Fujimoto, L. A. Wylie, and S. Saito, *ibid.* **58**, 1273 (1973); R. Calvo, S. B. Oseroff, and H. C. Abache, *ibid.* **72**, 760 (1980).
[25] M. Yokota and S. Koide, J. Phys. Soc. Jpn. **9**, 953 (1954).
[26] P. M. Richards and M. B. Salamon, Phys. Rev. B **9**, 32 (1974).
[27] M. C. G. Passeggi and R. Calvo, J. Magn. Res. **81**, 378 (1989).
[28] M. J. Hennesy, C. D. McElwee, and P. M. Richards, Phys. Rev. B **7**, 930 (1973).
[29] R. A. Tahir-Kheli and D. G. McFadden, Phys. Rev. **192**, 604 (1969).
[30] T. Wakamatsu, T. Hashiguchi, M. Nakano, M. Sorai, H. Suga, and Tan Zhi-cheng, Chin. Sci. Bull. **34**, 1795 (1989).
[31] C. M. Weeks, A. Cooper, and D. A. Norton, Acta Crystallogr. Sect. B **25**, 443 (1969).
[32] R. Calvo, H. Isern, and M. A. Mesa, Chem. Phys. **100**, 89 (1985).